

PAPER • OPEN ACCESS

## Assessment of the rehabilitation benefits by finite element method

To cite this article: A Dimitrescu *et al* 2019 *IOP Conf. Ser.: Mater. Sci. Eng.* **591** 012046

View the [article online](#) for updates and enhancements.

# Assessment of the rehabilitation benefits by finite element method

**A Dimitrescu, C Babis, O Chivu and L Dascalu**

Politehnica University of Bucharest, Faculty of Industrial Engineering and Robotics,  
Department of Quality Engineering and Industrial Technologies, Blvd. Splaiul  
Independentei, No. 202, 060021, Bucharest, Romania

E-mail: claudiubbs@gmail.com

**Abstract.** Cruciform fillet welded joints are found in many industrial applications. Welded structures are often subjected to load cycles due to loads that can vary in position and value. As a result of these loads, the phenomenon of fatigue occurs. Fatigue consists in the occurrence of failures, after applying a large number of load cycles, of loads below the yield limit of the material from which the structure is made. Fatigue mattempts have to be carried out over very long periods of time and are very expensive because of the expensive machines. A method by which the fatigue behavior of fillet welded joints can be predicted is the finite element method. The paper proposes to investigate by the finite element method, the fatigue life of some cruciform-fillet-welded specimens, making a comparison of two applied rehabilitation techniques.

## 1. Introduction

Due to the catastrophes that can be generated by fatigue failure of welded structures, research into their fatigue phenomena is of major international relevance. In this sense, there are extensive researches, among which we mention the fatigue tests of the welded joints, the factors influencing the fatigue life of the welded structures, the prediction of the fatigue life of the welded structures, the welding rehabilitation techniques of the welded joints in view increasing fatigue life and rising the sustainability curves [1-4].

Fatigue is described as the phenomenon of accumulating stresses and deformations that cause cracking and sometimes removal from operation by destroying structures as a result of applying variable loads in time like intensity and position, loads that have a value below the yield limit of the material from which the structure is made.

The mechanism of fatigue destruction includes 3 phases: initiation of the crack, crack growth and final rupture. The cracking initiation usually occurs on the surface of the material in the vicinity of a notch or stress concentrator. The phenomenon is explained by a sliding mechanism at the microscopic level determined by maximum shear stresses. When the load is applied, several grains will suffer plastic deformation due to the sliding of crystallographic planes. The mechanism includes only a few grains where those crystallographic planes have an unfavorable orientation relative to the maximum shear stress. When the applied load is changed, the planes that have slipped initially will not realise in the initial position due to the ecrusion effect so that the result at the microscopic level will be the appearance of some intrusions and extrusions on the surface of the material. The intrusions will behave like microcracks that determine the subsequent crack extension during the subsequent loading



cycles. In the second phase after the crack initiation was made inside a few grains, microscopic crack growth will extend the crack over a few grain boundaries. When the frontal cracking passes over a few grains, the crack will continue to grow in a perpendicular to the highest traction tension. In the crushing phase, the process is explained by a crack opening mechanism, smoothing its tip, followed by a crack closing mechanism and a tip sharpening along each loading cycle. After a complete cycle, the cracking front advanced with a small increment on the tired surface. The fracture from the third phase will occur when the crack becomes so large that the remaining cross section of the remaining bond is too small to transfer the stress of the loading cycle.

One of the factors that lead to a decrease in fatigue life time is stress concentrators.

The stress concentration is defined as a local increase in tension caused by a change in geometry or a discontinuity of the respective structural element. We often call “notches” these local geometric changes. In the area of the notch the peaks can be increased by 3 to 8 times the average nominal stress in the respective element. This magnitude is defined by the stress concentration factor noted in the literature with “K”. This is defined as the ratio of the local stress increase caused by the discontinuity and the nominal stress.

In this paper is analyzed with finite elements method the reduction of the stress concentrators and implicitly the increase of the fatigue lifetime by applying two rehabilitation techniques: grinding weld toe and WIG remelting weld toe. Both techniques determine by grinding or WIG remelting the modification of the geometric shape of the welding seam, in the sense of increasing the connection radius between the filler and the base material [5-8].

## 2. Experimental procedure

In this paper it was chosen to study the cross-welded joint on the one hand because it is very common with a high frequency of use in various engineering applications and on the other hand because it has a high potential for failure due to internal stresses accumulated during welding and stress concentrators.

The first stage of the experimental plan consists in the practical realization of a cruciform fillet welded sample (marked with B) in order to determine the geometrical characteristics of the welding seam both before and after the application of the two rehabilitation techniques “Grinding weld toe” and “WIG remelting weld toe”. In order to achieve the cruciform fillet welded joint we use three sheets with 10 mm of thickness as follows: a horizontal base plate with 150x350mm and two vertical plates with the dimensions of 70x350mm. The vertical plates are welded bilaterally resulting the cruciform fillet welded joint. The plates were made of steel type S 235 JR. The welding process used was in protective gas, using  $\text{Co}_2 + \text{Ar}$  gas. For welding it was used a cored wire with G3Si1 symbol according to EN-440, respecting the following parameters of the welding mode:

- Number of passages  $n = 3$
- Welding current intensity  $I_s = 230\text{-}235 \text{ A}$
- Voltage  $U_a = 20\text{-}22 \text{ V}$
- Wire speed  $= 0.5\text{cm/s}$
- Welding speed  $V_s = 5.5\text{m/min}$
- Linear Energy  $E_l = 8\text{kJ/cm}$

The initially obtained welding seams has a convex geometric shape, which means that there are large stress concentrators at the transition between the base and the filler material. Knowing that these stress concentrators drastically reduce fatigue lifetime, it is necessary to reduce them by increasing the connection radius between the base material and the filler material. In this respect, the cruciform sample was divided and cut into three equal parts along the welding bands. There was no rehabilitation technique applied to the first part, the second was applied to the "Grinding welding toe" technique and the third technique "WIG remelting welding toe" technique.

Next, three test pieces for fatigue tests were cut from each area: B2; B3 and B4 representing the first set, B5; B6 and B7 the second set and B8, B9 and B10 the third set. The cut specimens are intended for fatigue tests. This sub-stage is not the subject of this research, because in this paper there are no fatigue attempts, being only the simulation by the Ansys software.

In the second stage are taken pictures of the welding seams corresponding to those three zones with and without rehabilitation. The geometric characteristics of the welding cords are measured by a specialized software, which are listed in table 1.

Geometric elements K1, K2 and R of the welding seams of the specimens from sample B, are shown in table 1, where a is thickness of the welding seam, K1 and K2 are seam legs and R is the radius between seam and base material.

**Table 1.** Geometric elements of the welding seams for specimens sample B.

Zone	Specimen	a (mm)	K1=K2 (mm)	R (mm)
Without rehabilitation	B2; B3 and B4	5	7	0.5
Weld toe grinding	B5; B6 and B7	5	7	2
WIG remelting weld toe	B8; B9 and B10	5	10	4.5

In the third stage, with a computer-aided design program we realize the drawings of the three cruciform-specimens used to simulate fatigue tests, as shown in figure 1. We will have one representative specimen for each area of the cruciform fillet welded sample: the first with non-rehabilitated welding seams with unmodified geometry, the second with the modified geometry seams by the application of the “weld toe grinding technique” and the third with the seams with modified geometry by applying the “WIG remelting weld toe” rehabilitation technique.

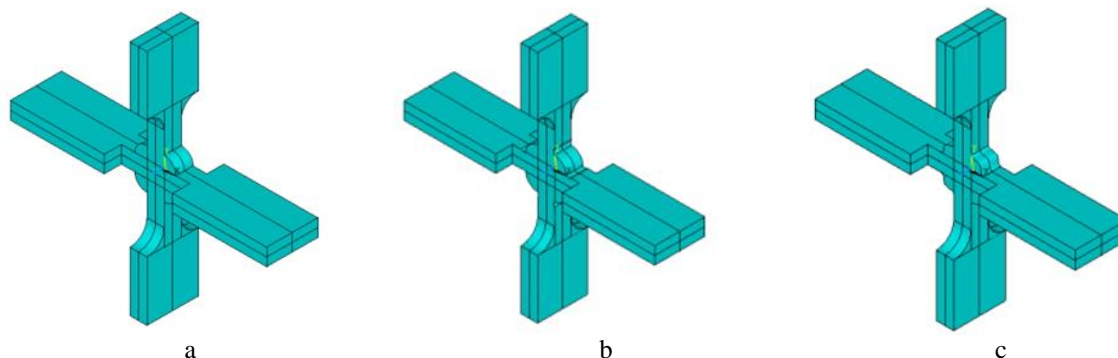


**Figure 1.** The tridimensional models of the specimens drawn in a computer assisted design program. (a) specimens B2, B3 and B4 without rehabilitation, (b) specimens B5, B6 and B7 with “grinding weld toe”, (c) specimens B8, B9 and B10 with “WIG remelting weld toe”.

In the fourth stage, for each representative sample described above, we realize the simulation of the fatigue tests. For this purpose, in order to obtain results to be compared one with each other, a symmetrical alternating compression tensioning cycle with a load frequency of 10Hz was used as the stress cycle. Fatigue attempts have been simulated because they require specialized equipment and very long time runs. Simulation of fatigue attempts includes several phases that will be presented below.

In order to simulate the fatigue phenomenon with the ANSYS software using the finite element analysis method, several steps have been completed and will be described below.

In the first step, from the preprocessor menu, we choose the element meshing and define material properties: Young’s modulus is 210GPa, Poisson’s ratio is 0.3, density 7850Kg/m<sup>3</sup>, Yield strength is 580MPa and the ultimate strength is 370Mpa.

Importing of the geometric patterns and meshing them into Ansys is shown in the figure 2.

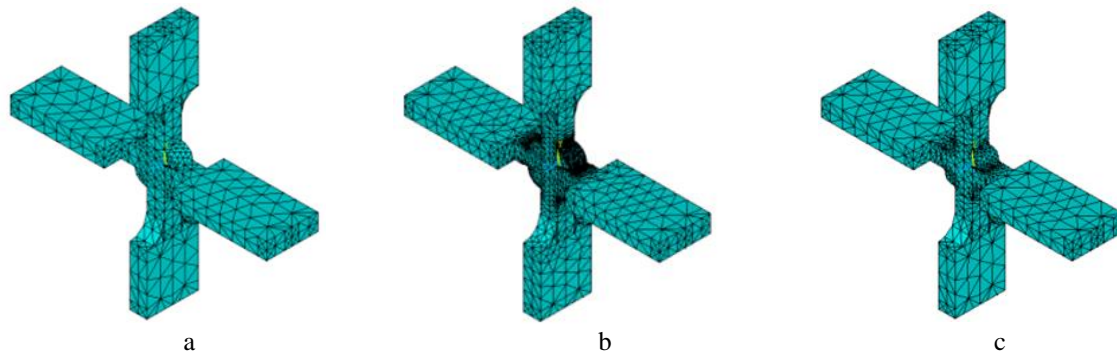


**Figure 2.** Importing and meshing volumes. (a) specimens B2, B3 and B4 without rehabilitation, (b) specimens B5, B6 and B7 with “grinding weld toe”, (c) specimens B8, B9 and B10 with “WIG remelting weld toe”.

The second step is enable the processor Solution and select Transient analysis. This phase, contain many steps. First load step is to comply with test conditions, constraint nodes specimen volumes and lower tensile force is applied in higher volumes nodes of the specimen. Also, we apply structural displacement on nodes as we can see in figure 3. In the second load step, we select volumes and nodes in the upper part of the specimen as we can see in figure 4 and apply successively tensile force of 14KN, 9KN, 7.5KN in these nodes in direction Fy.

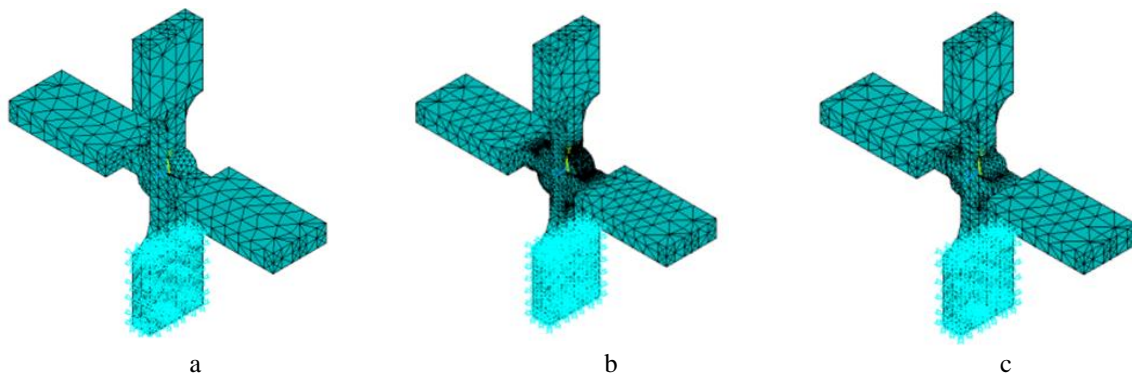


**Figure 3.** Constraint. (a) specimens B2, B3 and B4 without rehabilitation, (b) specimens B5, B6 and B7 with “grinding weld toe”, (c) specimens B8, B9 and B10 with “WIG remelting weld toe”

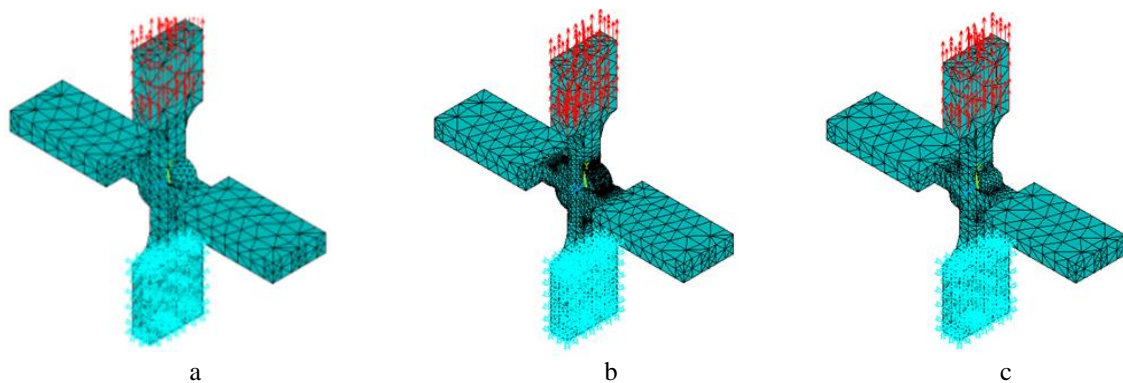


**Figure 4.** Applying tensile forces. (a) specimens B2, B3 and B4 without rehabilitation, (b) specimens B5, B6 and B7 with “grinding weld toe”, (c) specimens B8, B9 and B10 with “WIG remelting weld toe”.

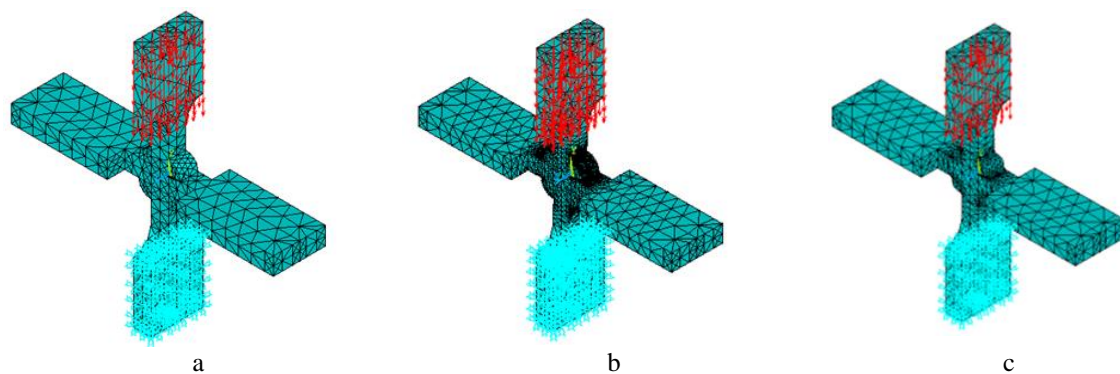


**Figure 5.** Applying compressive forces. (a) specimens B2, B3 and B4 without rehabilitation, (b) specimens B5, B6 and B7 with “grinding weld toe”, (c) specimens B8, B9 and B10 with “WIG remelting weld toe”.

In the third load step we select volumes and nodes in the upper part of the specimen as we can see in figure 5 and apply successively compressive force of -14KN, -7.5KN, -5KN in these nodes direction  $F_y$ . It was considered that all attempts were performed at the 10 Hz frequency, the stress cycle being a symmetrical alternating one, with the asymmetry coefficient  $R = -1$ , the stress being that of tension compression one. For the determination of the stress intensity, three variations of force were applied to each set of specimens, as follows: to the samples of set 1 without rehabilitation we apply to  $B2 \pm 14$  KN, to  $B3 \pm 7.5$  KN and to  $B4 \pm 5$  KN, to the specimens of set 2 with “grinding weld toe” we apply for  $B5 \pm 14$  KN, for  $B6 \pm 7.5$ KN, for  $B7 \pm 5$ KN and for third set of test specimens, with “WIG remelting weld toe”, we apply to  $B8 \pm 14$ KN, to  $B9 \pm 7.5$ KN and to  $B10 \pm 5$ KN

The third phase is Post processor. The stress intensity is presented in figure 6.

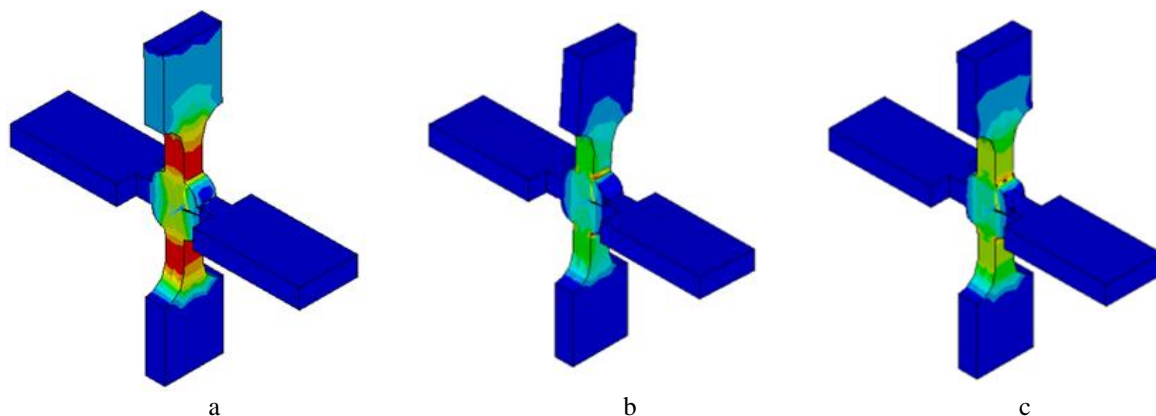


**Figure 6.** The stress intensity. (a) specimens B2, B3 and B4 without rehabilitation, (b) specimens B5, B6 and B7 with “grinding weld toe”, (c) specimens B8, B9 and B10 with “WIG remelting weld toe”.

In the stage 5 a mathematical prediction is performed using a mathematical predictive software, CurveExpert 1.4. In this issue we can determine on the basis of the experimental laboratory samples what can happen with these, under the same working conditions, but using other forces.

This prediction is very useful because in many cases fatigue attempts are long-term attempts to perform and thus we can streamline the pre-production periods in the process.

For example, we will consider the first set of the experimental samples, consisting of the B2, B3 and B4 specimens and the program used, generated 11 regression equations presented in figure 7.



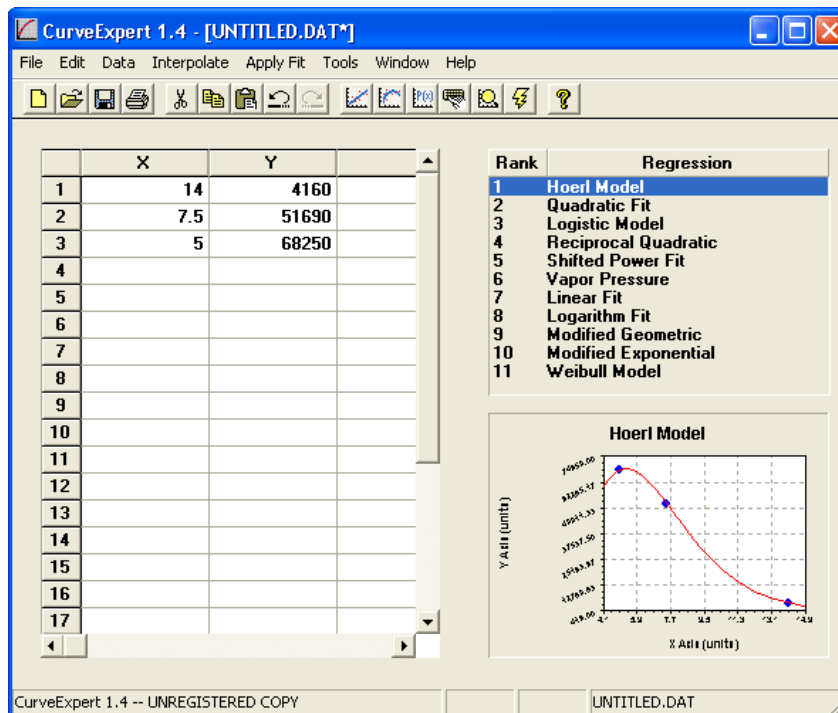


**Figure 7.** Generate regression equations.

From these, the Hoerl Model function fulfills the requirements: the standard error  $s = 0$  and the correlation coefficient  $R = 1$ , figure 8.

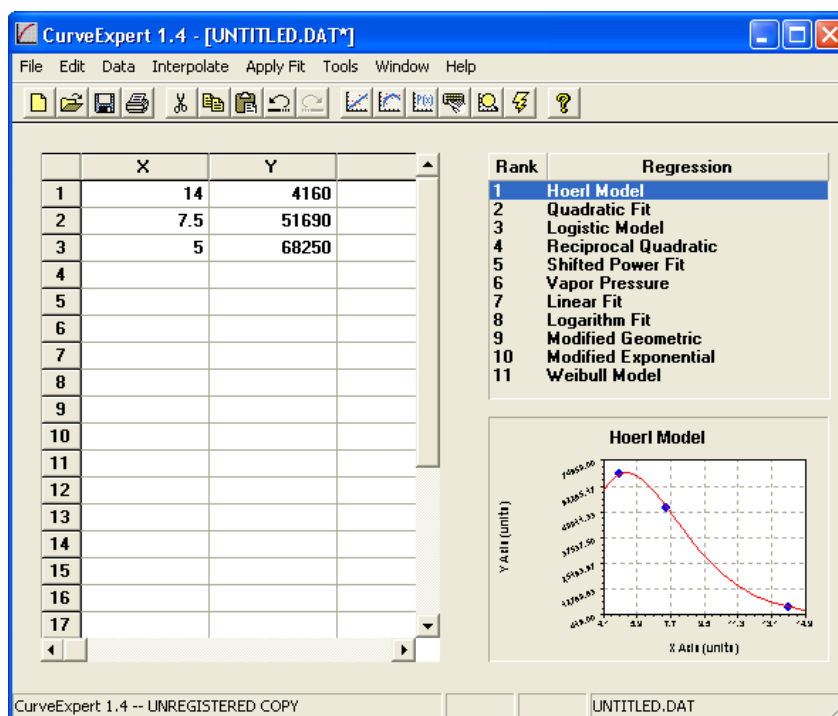


**Figure 8.** The graphical form of the Hoerl Model regression equation.

The equation has the algebraic shape shown in figure 9.

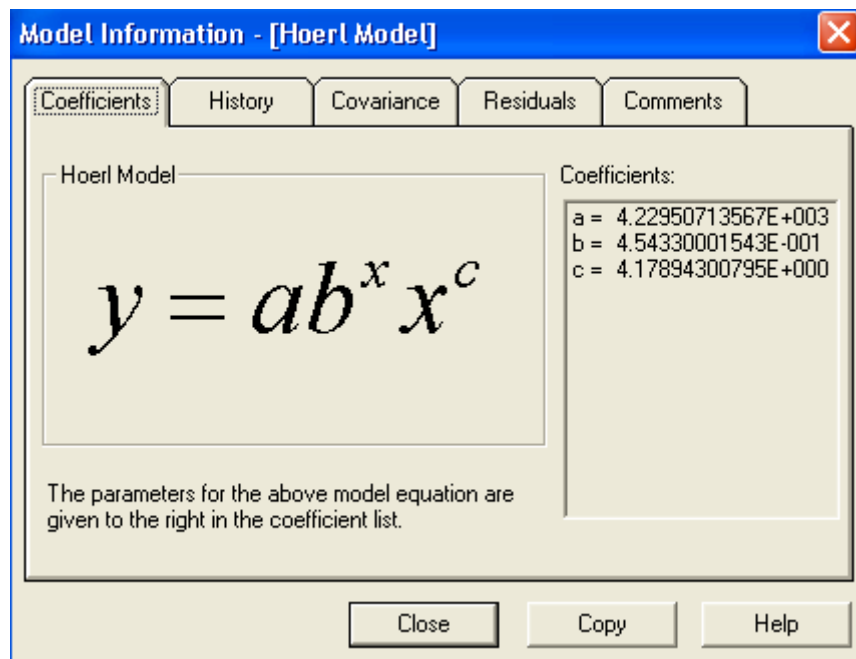


**Figure 9.** The algebraic form of the Hoerl Model equation.

The only disadvantage of the Hoerl Model regression equation is the residual inhomogeneity close to 14.9, as can be seen from figure 10.

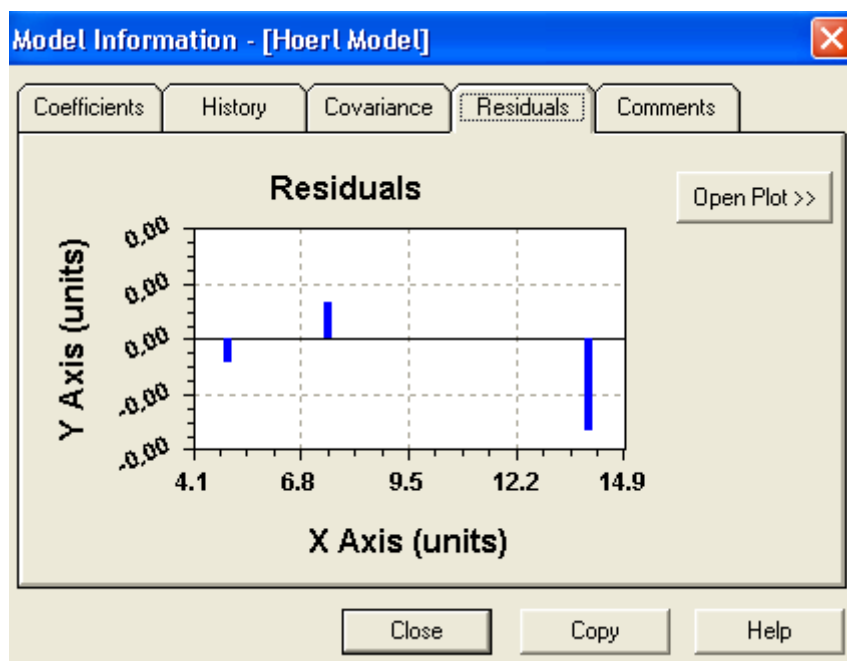


**Figure 10.** Residual scheme of the Hoerl Model equation.

### 3. Results and discussions

Forces applied to the specimens and results obtained from ANSYS analyses are presented centralized in table 2. The results obtained are almost the same with those obtained from experimental tests. The results of the experimental tests were presented in another paper.



**Table 2.** Results from ANSYS analyses.

No.	Rehabilitation technique	Mark	Frequency (Hz)	Force +/-Fi (kN)	Time (s)	Number of cycles until failure (N=t*f)
1	Without rehabilitation	B2	10	±14	416	4160
2		B3		±7.5	5169	51690
3		B4		±5	6825	68250
4	Grinding weld toe	B5		±14	603	6030
5		B6		±7.5	7495	74950
6		B7		±5	9287	92870
7	WIG remelting weld toe	B8		±14	1239	12390
8		B9		±7.5	15351	153510
9		B10		±5	19875	198750

#### 4. Conclusions

We notice that, with decreasing tensile stress on specimens B2, B3 and B4, increases the number of cycles up to failure. We mention that on specimens without reconditioning B2, B3 and B4, we have the highest value of the stress concentrator at the junction between the welding seam and the base material because of the smallest radius connecting seam to the base material, namely  $R = 0.5$  mm.

The specimen B5 on which we apply  $\pm 14$ KN, failed after 6030 cycles, B6 on which we have applied  $\pm 7.5$ KN failed after 74950 load cycles and B7 on which we have applied  $\pm 5$ KN failed after 92870 load cycles. We found an increase in the number of cycles compared to specimens homologous B2, B3 and B4. This is explained by the stress concentrator reduction at the top seam connection, by increasing the radius of 0.5 to 2 mm as shown in table 1.

We also observed that the specimen B8 that on which we have applied  $\pm 14$ KN, failure after 12390 cycles, the specimen B9 that we have applied  $\pm 7.5$ KN, failure after 153510 load cycles, and the specimen B10 that we have applied  $\pm 5$ KN failed after 198750 load cycles. We determinate an increase in the number of cycles compared to the homologous B5, B6 and B7 specimens. This is also explained by the stress concentrators reduction at the top seam according to table 2 by increasing the radius from 2 to 4.5mm.

To predict the fatigue failure cycles of the first set of specimens, the Hoerl Model function fulfills the requirements: the standard error  $s = 0$  and the correlation coefficient  $r = 1$ .

#### 5. References

- [1] Zhao-Ling W and Heng X 2017 Direct modeling of multi-axial fatigue failure for metals *International J. of Solids and Structures* **125** 216-231
- [2] Monika O, Peter P and Milan U 2017 Fracture mechanism differences created by fatigue and impact test *Materialstoday Proceedings* **4**(5) 5921-5924
- [3] Zeljko B, Siegfried S and Hinko W 2018 The effect of residual stresses on fatigue crack propagation in welded stiffened panels *Engineering Failure Analysis* **84** 346-357
- [4] Vikrant G, Sanjiwan B, Sagar I, Swapnil M and Lakade S 2017 Effect of Post Weld Toe Treatments on Fatigue Life of Welded Structures using FEA *Materialstoday Proceedings* **4** 1116-1126
- [5] Babis C, Amza G, Nitoi D, Chivu O and Apostolescu Z 2016 Innovative technology for rehabilitation of welded fillet joints, in order to increase the fatigue lifetime *Nano, Bio and Green Technologies for A Sustainable Future (International Multidisciplinary Scientific Geo Conf.)* **1** pp 183-190
- [6] Amza, G, Nitoi D, Babis C, Amza C and Apostolescu Z 2013 Influence of the Milling Weld Toe and WIG Remelting Reconditioning Technology to Welded Pieces in the Case of Fatigue Testing *Advances in Applied Materials and Electronics Engineering (Series: Advanced Materials Research)* **684** 362-366
- [7] Amza G, Babis C and Nitoi D 2014 The influence of the specific rehabilitation techniques "toegrindig" and "wig remelting" in case of welded structure *Metalurgia* **53** 71-74
- [8] Armando L, Rama I, Jose A, Carlos A and Branco G 2011 Fatigue behaviour of T welded joints rehabilitated by tungsten inert gas and plasma dressin *Materials and Design* **32** 4705-4713